


Cite this: *RSC Adv.*, 2019, 9, 13940

# Synergistic inhibition effect on the self-acceleration characteristics in the initial stage of methane/air explosion by CO<sub>2</sub> and ultrafine water mist

Bei Pei,<sup>a</sup> Shuangming Wei,<sup>a</sup> Liwei Chen,<sup>a</sup> Rongkun Pan,<sup>a</sup> Mingguo Yu<sup>\*b</sup> and Guoxun Jing<sup>\*a</sup>

Cellular instability is responsible for the self-acceleration of a flame, and such acceleration might cause considerable damage. This paper presents an experimental study on the inhibition effect of CO<sub>2</sub> and an ultrafine water mist on the self-acceleration characteristics of a spherical flame in the initial stage of a 9.5% methane/air explosion in a constant volume combustion bomb. Results showed that insufficient water mist enhanced the self-acceleration of the spherical flame and the intensity of the explosion; nevertheless, the synergistic inhibition effect of CO<sub>2</sub> and ultrafine water mist prevented enhancement of the explosion and significantly mitigated the self-acceleration of spherical flames, which observably delayed the appearance time of a cellular flame, and reduced the flame propagation speed, overpressure and the mean rate of pressure rise, indicating that suppression of flame self-acceleration could effectively mitigate the damage from a methane/air explosion. The reason for the synergistic effect was a result of a combination of physical suppression and chemical suppression: due to the preferential diffusion dilution effect of CO<sub>2</sub>, the initial flame speed was reduced, and the flame became thicker, which increased the evaporation time and quantity of droplets around the flame front, accordingly enhancing the cooling effect on the flame front. The increased flame thickness could withstand greater disturbance and inhibit the formation and development of a cellular flame. Meanwhile, CO<sub>2</sub> and H<sub>2</sub>O can also reduce the concentration of active radicals (O, H and OH) and reduce the reaction rate and combustion rate of a methane/air explosion.

Received 14th February 2019  
Accepted 24th April 2019

DOI: 10.1039/c9ra01148j

rsc.li/rsc-advances

## 1. Introduction

Methane/air explosion accidents often occur in the field of gas transportation and industrial production, posing a serious threat to the safety of human life and property. The flame front becomes unstable under the action of instabilities such as diffusional/thermal instability or hydrodynamic instability, increasing the contact area between the flame surface and the unburned gas, which causes the flame to self-accelerate.<sup>1–6</sup> This self-acceleration effect can affect the entire flame combustion process and cause more serious damage. Therefore, it is of great practical significance to limit the formation and growth of cellular flames in the initial stage of a methane/air explosion to reduce explosion hazards.

Due to the advantages of environmental protection and high cost-effectiveness, ultrafine water mist has been widely

considered by scholars for suppressing the explosion of combustible gases.<sup>7–9</sup> Previous research showed that ultrafine water mist suppressed a combustible gas explosion mainly through a physical effect.<sup>10–13</sup> Lentati *et al.*<sup>14</sup> and Yoshida *et al.*<sup>15</sup> found that ultrafine water mist not only had a physical inhibition effect but also a chemical inhibition effect. Cao *et al.*<sup>16</sup> found that ultrafine water mist could prevent the production of the main active radicals in a chain explosion reaction. Moreover, the particle size of the ultrafine water mist will affect the explosion suppression effect. Holborn *et al.*<sup>17</sup> found that the explosion suppression efficiency increased with a decrease in the particle size of the water mist. Modak *et al.*<sup>18</sup> studied the inhibition by fine water mist on a premixed methane/air flame. It was found that smaller diameter water mist was more effective than large diameter water mist. For the same net mass loading of water mist, there was a limit of 10 μm in diameter, and when the water mist diameter was less than or equal to 10 μm, it had the same suppression characteristics for a methane/air flame.

Meanwhile, Gieras *et al.*<sup>19</sup> and Cheikhraev *et al.*<sup>20</sup> found that the turbulence generated by water mist would accelerate flame

<sup>a</sup>Collaborative Innovation Center of Coal Safety Production of Henan Province, Henan Polytechnic University, Jiaozuo, Henan 454003, PR China

<sup>b</sup>State Key Laboratory of Coal Mine Disaster Dynamics and Control, Chongqing University, Chongqing 400044, PR China


propagation. Yu *et al.*<sup>21</sup> pointed out that adequate water mist could effectively reduce the explosion intensity, but it would increase the explosion intensity when the water mist was insufficient. Many scholars also improved ultrafine water mist to achieve a better suppression effect. Chelliah *et al.*<sup>22</sup> studied the effect of water mist with different additives (KOH/NaCl/NaOH) on methane/air explosion. The results indicated that water mist with chemical additives could significantly enhance the explosion suppression ability of water mist. However, the addition of chemical additives can also have negative factors, such as reducing the rate of evaporation during the interaction of the droplets with the flame. It is worth noting that our previous studies showed that a combination of nitrogen and ultrafine water mist could prevent the enhancement of a methane/air explosion caused by insufficient ultrafine water mist, and the inhibition effect was better than that of single inhibitor.<sup>23,24</sup>

Some scholars studied the effects of flame instability on spherically propagating flames under suppression by dilution gases. Wang *et al.*<sup>25</sup> investigated the laminar burning velocities of CO/H<sub>2</sub>/CO<sub>2</sub>/O<sub>2</sub> flames and the results showed that the cellular flame structure was promoted with an increase in hydrogen fraction and was suppressed with an increase in CO<sub>2</sub> fraction due to the combined effect of hydrodynamic and diffusive-thermal instability. Qiao *et al.*<sup>26</sup> carried out experiments on the effects of the four diluents of helium, argon, nitrogen and carbon dioxide with a dilution volume fraction of 0–40% on the laminar burning velocity of a hydrogen/air premixed flame, and the results showed that the order of four inert gases to reduce laminar burning velocity was: helium < argon < nitrogen < carbon dioxide. Xie *et al.*<sup>27</sup> compared the effect of CO<sub>2</sub> and H<sub>2</sub>O (water vapour) on the laminar burning characteristics of CO/H<sub>2</sub>/air mixtures at elevated pressures and pointed out that CO<sub>2</sub> and/or H<sub>2</sub>O weakened the hydrodynamic instability, but increased the thermal diffusion instability, and CO<sub>2</sub> dilution had a larger effect because of its lower effective Lewis number compared with H<sub>2</sub>O dilution.

From the above review, it seems that previous research on water mist suppression has focused mainly on the macroscopic suppression effect on flame propagation and overpressure waves. Furthermore, the influence of gas–liquid two-phase inhibitors on the self-acceleration characteristics of a flame in the initial stage of an explosion has not been investigated in the open literature. The objective of the present study is to illustrate the synergistic inhibition effect of gas–liquid two-phase inhibitors on the self-acceleration characteristics of cellular flames and the interaction between flame acceleration and pressure wave, which can provide guidance for preventing the acceleration of combustible gas explosions.

## 2. Experimental apparatus and procedures

The constant volume combustion bomb test system is shown in Fig. 1, which consists of a constant volume combustion bomb with three windows, a gas supply system, an ultrasonic

atomization system, a data acquisition and control system, an ignition system, an optical schlieren system and a high-speed camera system. The constant volume combustion bomb is a cylinder with a diameter of 290 mm and a length of 365 mm, which is made of welded stainless steel. The wall thickness of the combustion bomb is 30 mm and the pressure resistance is 2 MPa. In order to capture the flame propagation process, two finely machined optical quartz glass windows, with a diameter of 110 mm and a thickness of 50 mm were installed on either end of the combustion bomb. Another finely machined optical quartz glass window, with a diameter of 110 mm and a thickness of 50 mm was installed on the sidewall of the combustion bomb to determine the ignition time.

An MD-HF piezoresistive pressure sensor was located on the sidewall of the combustion bomb, with a measuring range of −0.1 to 1.0 MPa, a total error of 0.25%, and a dynamic response time of 1 ms. An RL-1 photodiode sensor was positioned outside the sidewall optical quartz glass window, as shown in Fig. 1. The signals from the pressure sensor and the photodiode sensor were recorded by a USB-1608FS Plus high-frequency data acquisition card, with a rate of 15 kHz. Ignition was achieved by high-voltage point discharge, and the output voltage was 6 kV with an ignition energy of 2.5 J. A pair of tungsten wire electrodes, with a 2 mm diameter, were positioned at the center of the combustion bomb, with a gap of 3 mm.

The gas supply system consisted of gas valves, pipes, three gas cylinders, a mass flow controller (MFC), a vacuum pump, and a precision digital pressure gauge. High-purity methane (≥99.99%) and CO<sub>2</sub> (≥99.99%) were supplied by two gas cylinders. The ultrasonic atomization system included mainly an ultrasonic atomization device, a sealed square water storage box, and an inlet and outlet pipe. The ultrasonic atomization device used a three-head copper atomizer, and the atomization chip operated at a frequency of 1700 kHz. The atomization rate of the ultrasonic atomizer was 4.2 g min<sup>−1</sup>, which was measured in advance by a precision balance. According to the atomization rate, the concentration of ultrafine water mist could be ensured by adjusting the atomization time. In the present experiment, the mass concentration of ultrafine water mist was set as follows: 58.3 g m<sup>−3</sup>, 174.9 g m<sup>−3</sup>, 262.5 g m<sup>−3</sup> or 350 g m<sup>−3</sup> by controlling the atomization time. As shown in Fig. 2, the droplet sizes of the ultrasonic water mist in the experiment range from 0 to 20 μm, which were measured by a Phase Doppler Anemometer (PDA) produced by the Dantec Dynamics A/S company. The Sauter mean diameter  $D_{32}$  was 6.3 μm and the standard deviation was lower than 5%. The initial pressure of the mixtures was 101 kPa, and the initial temperature was 283 K.

Before preparing the gas mixture, the combustion bomb was vacuumed to −0.096 MPa and confirmed as being well-sealed. Next, a methane/air premixed gas was prepared with a fraction of 9.5% in the combustion chamber based on Dalton's law of partial pressures. The carbon dioxide was then taken in according to the ratio. It should be emphasized that the ultrafine water mist was taken into the combustion bomb with the air, and the intake speed was controlled by the mass flow controller. When the ultrafine water mist was taken into the



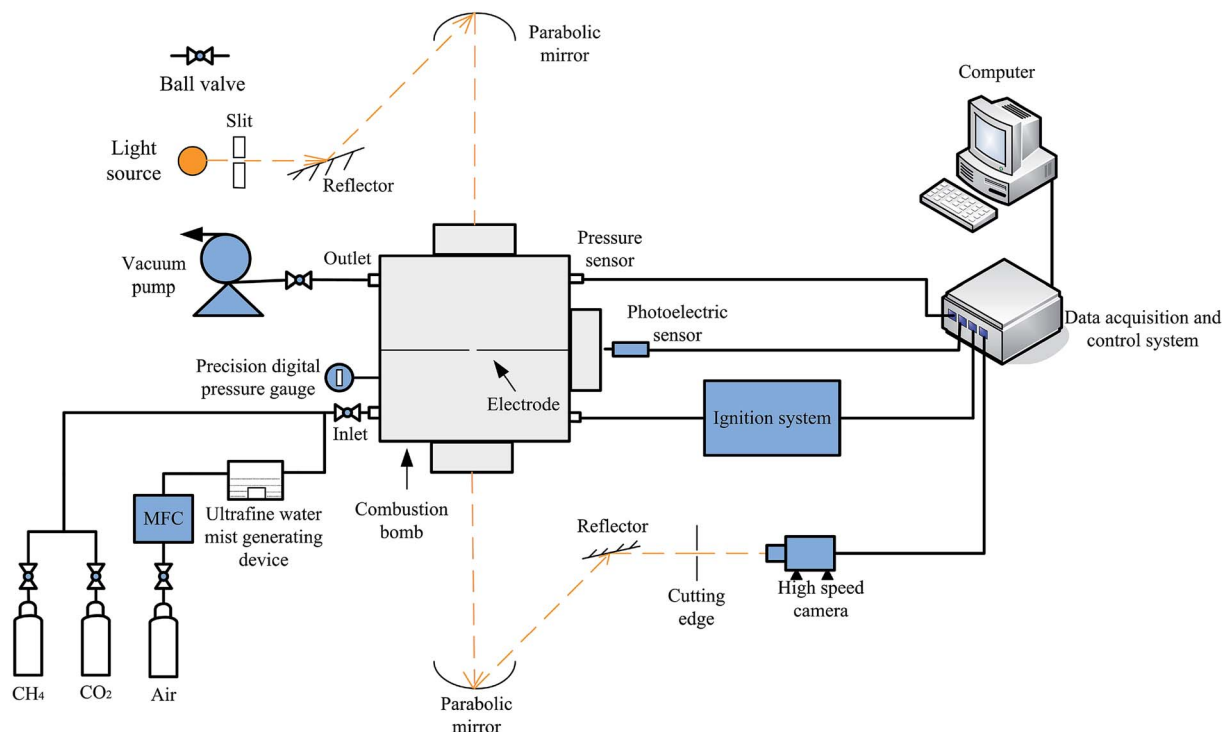


Fig. 1 Schematic of experimental apparatus.

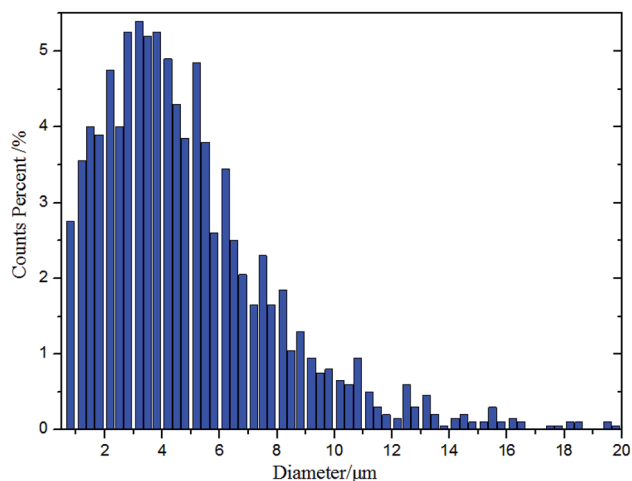


Fig. 2 Particle size distribution diagram of ultrafine water mist.

vessel, the mixture needed to stand for 30 s before ignition, in order to mix the ultrafine water mist with the mixture gas. After ignition, the explosion flames were observed by a schlieren system (CQW300) through two quartz windows and recorded by a high-speed camera (High Speed Star 4G, made by Lavision), which was operated at 2000 fps with  $1280 \times 800$  pixel image resolution. In order to ensure the reliability and repeatability of the experimental data, each experiment was performed at least 5 times.

### 3. Results and discussions

#### 3.1. Effect of $\text{CO}_2$ on the self-acceleration characteristics of a 9.5% methane/air explosion spherical flame

The developing process of combustible gas explosion sphere flame propagation can be divided into laminar flame, self-similar flame, self-acceleration flame and self-turbulence flame.<sup>28</sup> The cellular flame formation could be attributed to diffusional/thermal instability and hydrodynamic instability.<sup>28</sup> The developing process of a 9.5% methane/air explosion spherical flame is shown in Fig. 3. It can be seen that when the premixed gas was ignited, a spherical flame was formed which propagated outward quickly in a laminar state. The spherical flame front was smooth and reached the edge of the window at about 24 ms. However, since methane is a low-active combustible gas with a low burning rate, and the temperature of the methane/air flame was not too high, the flame front did not generate a cellular flame before reaching the edge of the window. As the spherical flame continued to propagate, the surface of the flame produced irregular cracks at a time of 63 ms. These cracks later quickly formed into a homogeneous and fully cellular flame at a time of 83 ms. Therefore, the authors

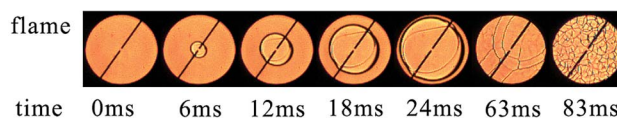


Fig. 3 Development process of a 9.5% methane/air spherical flame.



believe that this may be due to the combined effect of the activity of the combustible gas and the instability of the flame.

Fig. 4 presents the inhibition effect of different fractions of CO<sub>2</sub> on the propagation progress of the spherical flame of a 9.5% methane/air explosion. First, with an increase in the volume fraction of CO<sub>2</sub>, the radius of the spherical flame decreased significantly at the same time after ignition, which showed that CO<sub>2</sub> had an obvious inhibition effect on the propagation of the methane/air explosion; the higher the CO<sub>2</sub> fraction, the more obvious the inhibition effect. This finding was obtained because the methane explosion was essentially a chain reaction process, while CO<sub>2</sub> diluted the premixed gas, inhibited the dissociation of activated radicals, reduced the concentration of activated radicals, and thus reduced the flame propagation speed.<sup>29</sup> Second, CO<sub>2</sub> also had an obvious effect on the structure of the methane/air explosion spherical flame. Compared to Fig. 3, the 9.5% methane/air explosion spherical flame generated only a few cracks on the flame front at a time of 12 ms formed by the electrodes. With an added 2% CO<sub>2</sub>, the number of flame surface cracks was reduced. The fully cellular flame did not appear until 100 ms. Lastly, with the increase in CO<sub>2</sub> fraction, the flame front became smoother. This may be because CO<sub>2</sub> reduced the temperature and the combustion reaction rate, and hence the flame propagation speed decreased, which is an important parameter for characterizing hydrodynamic instability. It is worth noting that when the CO<sub>2</sub> volume fraction was greater than 14%, the cellular flame disappeared during the propagation progress of the spherical flame, and the flame appeared to float upward. When the CO<sub>2</sub> fraction increased to 18%, the phenomenon of floating upward became more serious, forming an ellipsoidal flame front. This was caused by the performance of the flame buoyancy instability, which was due to the slow speed of flame propagation. The reason for this phenomenon is that the density of mixed gas in the burned area was smaller than the density of the premixed gas in the unburned area.<sup>30</sup> Under the effect of buoyancy, the propagation speed of the upper flame was greater than the lower part. Therefore, the flame floated upward.

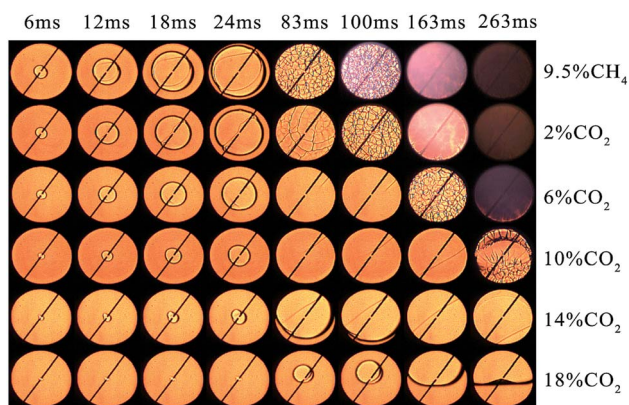


Fig. 4 Inhibition effect of different fractions of CO<sub>2</sub> on the propagation progress of a 9.5% methane/air spherical flame.

With the spherical flame propagating outward, the radius of the flame gradually increases, and the front of the flame will have a cellular structure at a certain moment. The cellular structure in the front of the flame will increase the contact area with the unburned gas, which will increase the combustion rate and accelerate the flame.<sup>3</sup> Therefore, the appearance time of the cellular flame can also reflect the time when the spherical flame starts to self-accelerate. Fig. 5 presents the inhibition effect of CO<sub>2</sub> on the relationship between the appearance time of the cellular flame and the overpressure of the 9.5% methane/air explosion spherical flame. It can be seen that for the 9.5% methane/air explosion, the spherical flame appeared in the cell structure at 83 ms, and the overpressure peak and the mean rate of pressure rise were 0.66 MPa and 3.0 MPa s<sup>-1</sup>, respectively. The mean rate of pressure rise is the maximum explosion pressure  $p_{\max}$  minus the initial pressure  $p_0$  divided by the time when the maximum explosion pressure appears.<sup>31</sup>

$$\nu = \frac{p_{\max} - p_0}{t_{p_{\max}}} \quad (1)$$

When 10% CO<sub>2</sub> was added, the appearance time of the cellular flame was delayed to 263 ms and was increased by 216.9% compared to the 9.5% methane/air explosion. It is interesting that there was no cellular flame during the whole explosion process when the fraction of CO<sub>2</sub> was greater than 14%. When 18% CO<sub>2</sub> was added, the peak overpressure and the mean rate of pressure rise decreased by 37.9% and 90%, respectively. It can be seen that with the increase in CO<sub>2</sub> volume fraction, the appearance time of the cellular flame gradually increased and caused the flame to float upwards, while the overpressure peak and the mean rate of pressure rise decreased. This finding indicates that a fraction of 14% CO<sub>2</sub> is necessary for a better inhibition effect on the initial propagation of the methane/air explosion. Furthermore, when 22% CO<sub>2</sub> was added, the premixed gas could not be ignited, indicating that the methane/air mixture was made completely inert.

### 3.2. Effect of ultrafine water mist on the self-acceleration characteristics of a 9.5% methane/air explosion spherical flame

Fig. 6 presents the inhibition effect of different mass concentrations of ultrafine water mist on the propagation process of the spherical flame of the 9.5% methane/air explosion. First, it can be seen that the flame radius first increased and then decreased with the increase in the mass concentration of ultrafine water mist. It is worth mentioning that under a mass concentration of 58.3 g m<sup>-3</sup> of ultrafine water mist, the radius of the spherical flame was bigger than that of the 9.5% methane/air explosion at the same time after ignition. Meanwhile, the time when the flame front was fully cellular was advanced to 80 ms, indicating the acceleration of the flame propagation. This is because the ultrafine water mist had a significant effect on the explosion flame front and changed the flow structure of the explosion flame, increasing the burning area,





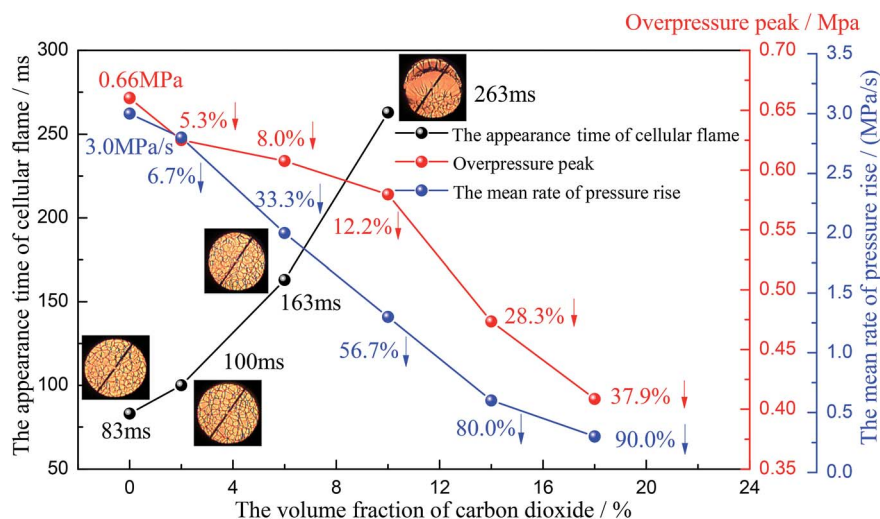


Fig. 5 Inhibition effect of CO<sub>2</sub> on the relationship between the appearance time of the cellular flame and overpressure of the 9.5% methane/air explosion spherical flame.

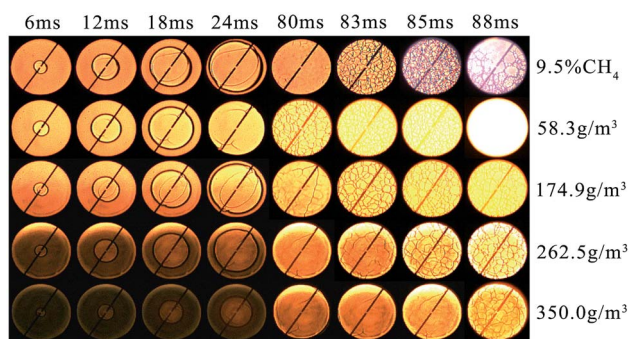


Fig. 6 Inhibition effect of different ultrafine water mist mass concentrations on the propagation of a 9.5% methane spherical flame.

and accelerating the heat transfer and mass transfer process between the flame front and the unburnt gas. Hence, due to an insufficient amount of ultrafine water mist, the cooling effect was so weak that the explosion was enhanced.

Second, when the mass concentration of ultrafine water mist was greater than 174.9 g m<sup>-3</sup>, the flame radius gradually decreased at the same time after ignition, indicating that the flame propagation speed was reduced gradually. Besides, with the increase in the mass concentration of ultrafine water mist, the size of the cellular flame got larger and larger. Meanwhile, the appearance time of the uniform large cellular flame was gradually delayed. This is because under the suppression of ultrafine water mist, the thickness of the flame front and the preheating area increased owing to its high latent heat of evaporation. Hence, the flame front could endure a small disturbance, and only large wrinkles were produced on the flame surface. Therefore, the ultrafine water mist mass concentration was an important factor influencing the explosion suppression effect. When the water mist was insufficient, it would promote the self-acceleration of the spherical explosion flame; in contrast, the self-acceleration of the cellular flame

would be effectively inhibited when the mass concentration of ultrafine water mist was sufficient.

Lastly, the brightness of the flame increased clearly under the effect of the ultrafine water mist. This may be because the ultrafine water mist rapidly decomposed at high temperature, generating free radicals such as H and undergoing a reforming reaction with methane, which ultimately led to an increase in the brightness of the flame.

Fig. 7 presents the inhibition effect of ultrafine water mist on the relationship between the appearance time of the cellular flame and overpressure of the 9.5% methane/air explosion spherical flame. With the increase in the ultrafine water mist mass concentration, the appearance time of the cellular flame first decreased and then increased; while the overpressure peak and the mean rate of pressure rise first increased and then decreased. As with a mass concentration of 58.3 g m<sup>-3</sup> of ultrafine water mist, the appearance time of the cellular flame was advanced by 80 ms. At the same time, the overpressure peak and the mean rate of pressure rise also increased by 4.5% and 30%, respectively. With the increase in the mass concentration of ultrafine water mist, the appearance time of the cellular flame was gradually delayed, and the overpressure peak and the mean rate of pressure rise also decreased.

Nevertheless, compared to Fig. 5, with the increase in CO<sub>2</sub> volume fraction, the appearance time of the cellular flame was significantly prolonged; even when the CO<sub>2</sub> volume fraction was greater than 14%, the cellular flame disappeared. It is important to point out that the decrease in the mean rate of pressure rise is much bigger than that of ultrafine water mist. Xie *et al.*<sup>27</sup> pointed out that CO<sub>2</sub> dilution showed a higher suppressing effect on hydrodynamic instability than that of H<sub>2</sub>O (water vapour); therefore, CO<sub>2</sub> had a greater influence on the cellular flame, which is consistent with our present work. These results also clearly stated that there was a corresponding relationship between flame acceleration and the mean rate of pressure rise.



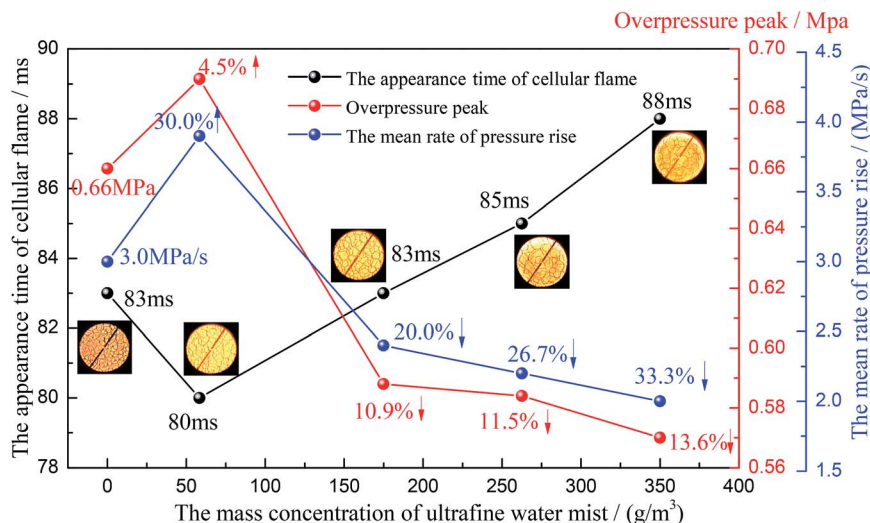


Fig. 7 Inhibition effect of different ultrafine water mist mass concentrations on the relationship between the appearance time of the spherical flame and explosion overpressure of a 9.5% methane/air spherical flame.

The inhibition of the formation of flame acceleration can mitigate the damage of explosion overpressure.

### 3.3. Effect of CO<sub>2</sub>–ultrafine water mist on self-acceleration characteristics of a 9.5% methane/air explosion spherical flame

Fig. 8 presents the combination inhibition effect of 174.9 g m<sup>-3</sup> ultrafine water mist and different volume fractions of CO<sub>2</sub> on the initial propagation process of a 9.5% methane/air explosion spherical flame. First, with an increase in the CO<sub>2</sub> volume fraction, the flame radius obviously decreased at the same time after ignition. Second, it can be seen that the flame surface became smoother with the combined effect of CO<sub>2</sub> and ultrafine water mist. Meanwhile, with the increase in CO<sub>2</sub> volume fraction, the appearance time of the cellular flame was gradually prolonged further. For example, under the combined effect of 10% CO<sub>2</sub> and an ultrafine water mist of 174.9 g m<sup>-3</sup>, there were only a few bigger folds on the flame front, and the flame began

to float upward sooner. When the volume fraction of CO<sub>2</sub> was greater than 14%, there was no wrinkle on the flame front during the propagation progress of the spherical flame, and the spherical flame floated upward in a more pronounced way, and the shape of the flame became ellipsoidal.

Fig. 9 illustrates the combined inhibition effect of 174.9 g m<sup>-3</sup> ultrafine water mist and different volume fractions of CO<sub>2</sub> on the relationship between the appearance time of a 9.5% methane/air spherical cellular flame and explosion overpressure. As is shown in Fig. 9, under the combined effect of CO<sub>2</sub> and an ultrafine water mist, the appearance time of the cellular flame was significantly delayed, and the overpressure peak and the mean rate of pressure rise also obviously decreased. For example, when 6% CO<sub>2</sub> and 174.9 g m<sup>-3</sup> ultrafine water mist were used alone, the appearance times of the cellular flame were 163 and 83 ms, respectively, and the overpressure peak and the mean rate of pressure rise decreased by 8% and 33.3%, and 10.9% and 20%, respectively; while under the combined effect, the appearance time of the cellular flame was delayed to 180 ms, the size of the cellular flame increased further, and the overpressure peak and the mean rate of pressure rise decreased by 13.2% and 55.3%, indicating the enhancement of the suppression effect on the interaction between flame acceleration and pressure wave. With the increase in the fraction of CO<sub>2</sub> and 174.9 g m<sup>-3</sup> ultrafine water mist, the synergistic inhibition effect of gas–liquid two-phase inhibitors on the initial propagation progress of a 9.5% methane/air explosion spherical flame gradually improved.

The mechanism of synergistic inhibition of CO<sub>2</sub> and ultrafine water mist on the self-acceleration of methane/air explosion spherical flame is shown in Fig. 10. On one hand, the preferential diffusion and dilution of CO<sub>2</sub> can reduce the initial flame propagation velocity of the flame and the thermal expansion ratio of the flame front, increasing the thickness of the flame front. It is beneficial to prolong the residence time and quantity of ultrafine water mist around the front of the

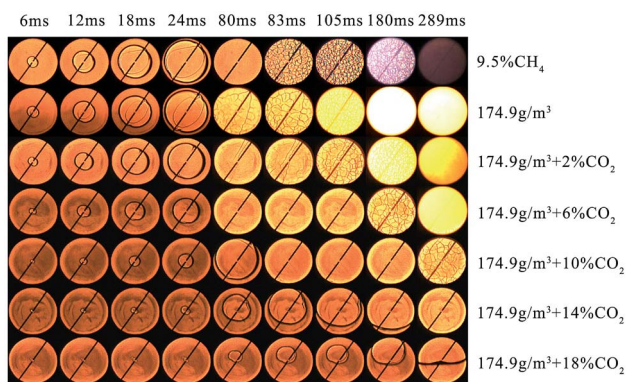


Fig. 8 Combined inhibition effect of 174.9 g m<sup>-3</sup> ultrafine water mist and different volume fractions of CO<sub>2</sub> on the initial propagation process of a 9.5% methane/air explosion spherical flame.

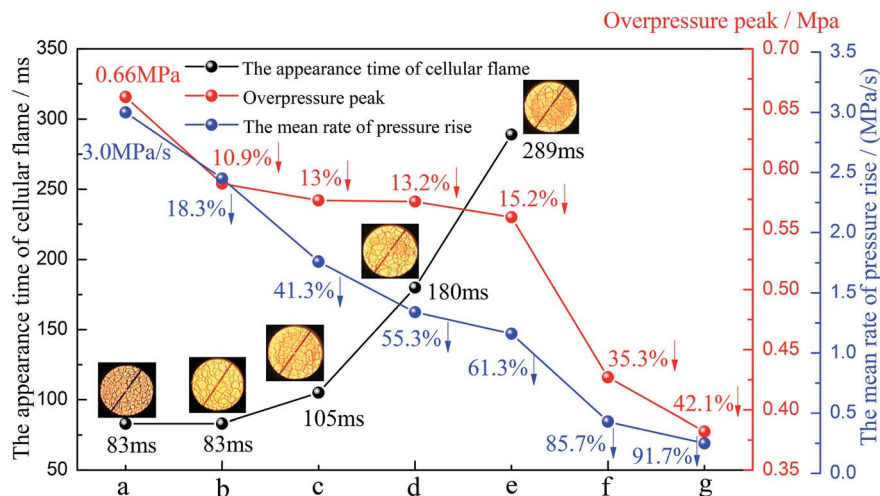


Fig. 9 Combined inhibition effect of  $174.9 \text{ g m}^{-3}$  ultrafine water mist and different volume fractions of  $\text{CO}_2$  on the relationship between the appearance time of a 9.5% methane/air spherical flame and explosion overpressure. ((a) 9.5% $\text{CH}_4$ , (b)  $174.9 \text{ g m}^{-3}$ , (c)  $174.9 \text{ g m}^{-3} + 2\%\text{CO}_2$ , (d)  $174.9 \text{ g m}^{-3} + 6\%\text{CO}_2$ , (e)  $174.9 \text{ g m}^{-3} + 10\%\text{CO}_2$ , (f)  $174.9 \text{ g m}^{-3} + 14\%\text{CO}_2$ , (g)  $174.9 \text{ g m}^{-3} + 18\%\text{CO}_2$ ).

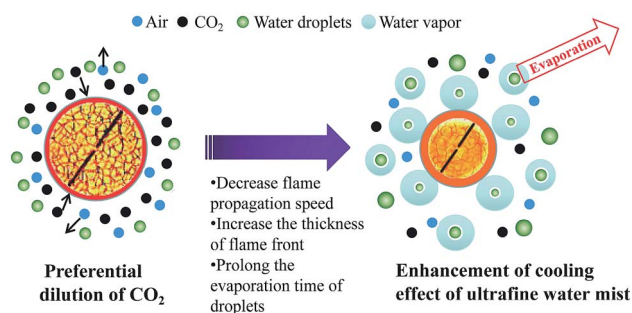
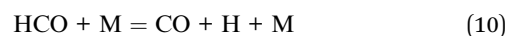
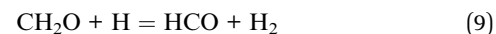
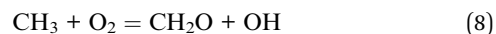
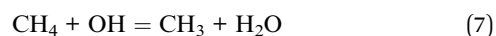
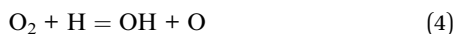
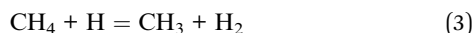


Fig. 10 Synergistic inhibition mechanism of  $\text{CO}_2$  and ultrafine water mist on the self-acceleration of a methane/air explosion spherical flame.

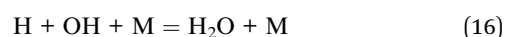
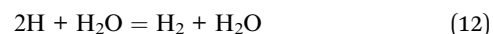
flame, significantly improving the cooling effect of the ultrafine water mist on the flame front. On the other hand, when the flame thickness increased to a certain extent, which enabled it to withstand greater disturbances this was not conducive to the formation and development of a cellular flame. That is the reason for the cellular flame disappearing under the combined effect of 14%  $\text{CO}_2$  and an ultrafine water mist of  $174.9 \text{ g m}^{-3}$ .

Lastly, owing to  $\text{CO}_2$  being one of the products of methane/air explosion reaction, adding  $\text{CO}_2$  could affect the direction of the reaction. Qiao *et al.*<sup>33</sup> simulated the chemical inhibition mechanism of  $\text{CO}_2$  on the methane/air explosion reaction with Chemkin. The simplified methane/air explosion reaction process is as follows:



They found that  $\text{CO}_2$  could be converted to  $\text{CO}$  through the reaction ( $\text{CO} + \text{OH} = \text{H} + \text{CO}_2$ ,  $\text{H}_2\text{O} + \text{CO} = \text{H}_2 + \text{CO}_2$ ), which would capture hydrogen radicals, while in the methane/air explosion reaction process,  $\text{H}$  and oxygen combine to form oxygen radicals and  $\text{OH}$ , which was the most important chain-branching reaction, resulting in a reduction in the concentration of key active radicals (such as  $\text{O}$ ,  $\text{H}$  and  $\text{OH}$ ) and thus reducing the flame propagation velocity.

Yoshida *et al.*<sup>34</sup> simulated the chemical inhibition mechanism of  $\text{H}_2\text{O}$  on methane/air explosion action with Chemkin. The reaction chain process of a methane/air explosion after adding  $\text{H}_2\text{O}$  is as follows:



From reactions (12) and (16), it can be seen that when water participates in the explosion reaction, it will capture hydrogen atoms and reduce the concentration of  $\text{H}$  with the highest





activity; meanwhile acting as the third body, H and OH combine to form  $\text{H}_2\text{O}$ , resulting in the continuous consumption of H and OH and suppressing the chain reaction of the methane/air explosion.

In summary, the synergistic inhibition effect of gas-liquid two-phase inhibitors is the result of a combination of physical suppression and chemical suppression. The present work also indicated that the characteristics of self-acceleration of the spherical flame could be greatly suppressed under the inhibition of gas-liquid two-phase inhibitors, which was of great significance for mitigating the damage of a methane/air explosion.

## 4. Conclusions

Spherical flames will spontaneously form cellular structures, resulting in flame acceleration due to an increase in flame surface area,<sup>32</sup> and when positive feedback is formed between the pressure wave and flame acceleration, considerable damage will happen. The damage caused by an explosion is mainly reflected by explosion overpressure, the rate of pressure rise and flame propagation speed. The present study investigated the synergistic inhibition effect of gas-liquid two-phase inhibitors on the self-acceleration characteristics of a methane/air explosion spherical flame and the interaction between flame acceleration and the pressure wave. The conclusions are as follows:

(1) The fraction of  $\text{CO}_2$  is an important factor affecting the inhibition effect. With an increase in  $\text{CO}_2$  volume fraction, the flame propagation speed of the spherical flame, the overpressure peak and the mean rate of pressure rise are gradually reduced, and the appearance time of the cellular flame is gradually delayed. When the  $\text{CO}_2$  volume fraction is greater than 14%, the cellular flame will disappear. This indicates that an adequate quantity of  $\text{CO}_2$  will better inhibit flame self-acceleration of a methane/air explosion.

(2) Insufficient ultrafine water mist will enhance flame instability and promote the self-acceleration of the spherical explosion flame. However, with an increase in the mass concentration of the ultrafine water mist, the appearance time of the cellular flame is gradually delayed; the spherical flame propagation speed, overpressure and the mean rate of pressure rise of 9.5% methane/air explosion are also gradually reduced.

(3) The combination of  $\text{CO}_2$  and ultrafine water mist can avoid the enhancement of a 9.5% methane/air explosion induced by insufficient water mist, and significantly reduce the flame propagation speed, peak overpressure, and the mean rate of pressure rise. Meanwhile, the appearance time of the cellular flame is obviously delayed, and the size of the cellular flame increases significantly. It can be concluded that the combined inhibition of  $\text{CO}_2$  and ultrafine water mist can significantly reduce the instability of the flame and significantly mitigate the self-acceleration of a 9.5% methane/air explosion spherical flame.

The synergistic inhibition mechanism of  $\text{CO}_2$ -ultrafine water mist on the self-acceleration of a 9.5% methane/air explosion spherical flame is a result of a combination of physical suppression and chemical suppression. For physical

suppression, under the preferential diffusion dilution effect of  $\text{CO}_2$ , the flame propagation speed is reduced and the flame becomes thicker, which prolongs the evaporation time of droplets around the flame front and enhances the cooling effect on the flame front. Therefore, there is a phase coupling inhibition effect of gas-liquid two-phase inhibitors. For chemical suppression,  $\text{CO}_2$  and  $\text{H}_2\text{O}$  can reduce the concentration of active radicals, such as O, H and OH, and hence the reaction rate and combustion rate of the methane/air explosion are reduced.

Moreover, the increased thickness of the flame front enable it to withstand greater disturbance and inhibit the formation and development of a cellular flame, resulting in significant suppression of flame self-acceleration, which is good for mitigating the damage of a methane/air explosion.

## Conflicts of interest

There are no conflicts to declare.

## Acknowledgements

This paper was financially supported by the research fund provided by the National Scientific Foundation of China (No. 51604095) and a project funded by the China Postdoctoral Science Foundation (No. 2018M630818), National key R&D plan (No. SQ2018YFC080003), and Postdoctoral research grant in Henan Province (No. 001802023), and Funding Scheme for Young Key Teachers of Henan University of Technology (No. 2018XQG-01).

## References

- 1 Y. Xie, J. Wang, X. Cai and Z. Huang, Self-acceleration of cellular flames and laminar flame speed of syngas/air mixtures at elevated pressures, *Int. J. Hydrogen Energy*, 2016, **41**(40), 18250–18258.
- 2 T. Katsumi, T. Aida, K. Aiba and S. Kadowaki, Outward propagation velocity and acceleration characteristics in hydrogen-air deflagration, *Int. J. Hydrogen Energy*, 2017, **42**(11), 7360–7365.
- 3 F. Wu, G. Jomaas and C. K. Law, An experimental investigation on self-acceleration of cellular spherical flames, *Proc. Combust. Inst.*, 2013, **34**(1), 937–945.
- 4 Y. Li, M. Bi, B. Li, Y. Zhou and W. Gao, Effects of hydrogen and initial pressure on flame characteristics and explosion pressure of methane/hydrogen fuels, *Fuel*, 2018, **233**, 269–282.
- 5 B. Nie, L. Yang, B. Ge, J. Wang and X. Li, Chemical kinetic characteristics of methane/air mixture explosion and its affecting factors, *J. Loss Prev. Process Ind.*, 2017, **49**, 675–682.
- 6 C. Wang, S. Wu, Y. Zhao and E. K. Addai, Experimental investigation on explosion flame propagation of  $\text{H}_2$ - $\text{O}_2$  in a small scale pipeline, *J. Loss Prev. Process Ind.*, 2017, **49**, 612–619.





- 7 F. Wang, M. Yu, X. Wen, H. Deng and B. Pei, Suppression of methane/air explosion in pipeline by water mist, *J. Loss Prev. Process Ind.*, 2017, **49**, 791–796.
- 8 X. Cao, J. Ren, Y. Zhou, Q. Wang, X. Gao and M. Bi, Suppression of methane/air explosion by ultrafine water mist containing sodium chloride additive, *J. Hazard. Mater.*, 2015, **285**, 311–318.
- 9 Y. Liang and W. Zeng, Numerical study of the effect of water addition on gas explosion, *J. Hazard. Mater.*, 2010, **174**(1–3), 386–392.
- 10 D. A. Schwer and K. Kailasanath, Numerical simulations of the mitigation of unconfined explosions using water-mist, *Proc. Combust. Inst.*, 2007, **31**(2), 2361–2369.
- 11 P. G. Holborn, P. Battersby, J. M. Ingram, A. F. Averill and P. F. Nolan, Modelling the mitigation of lean hydrogen deflagrations in a vented cylindrical rig with water fog, *Int. J. Hydrogen Energy*, 2012, **37**(20), 15406–15422.
- 12 X. Cao, J. Ren, M. Bi, Y. Zhou and Y. Li, Experimental research on the characteristics of methane/air explosion affected by ultrafine water mist, *J. Hazard. Mater.*, 2017, **324**, 489–497.
- 13 R. Ananth, H. D. Willauer, J. P. Farley and F. W. Williams, Effects of Fine Water Mist on a Confined Blast, *Fire Technol.*, 2012, **48**(3), 641–675.
- 14 A. M. Lentati and H. K. Chelliah, Physical, thermal, and chemical effects of fine-water droplets in extinguishing counterflow diffusion flames, *Symp. (Int.) Combust.*, [Proc.], 1998, **27**(2), 2839–2846.
- 15 A. Yoshida, T. Okawa, W. Ebina and H. Naito, Experimental and numerical investigation of flame speed retardation by water mist, *Combust. Flame*, 2015, **162**(5), 1772–1777.
- 16 X. Cao, J. Ren, M. Bi, Y. Zhou and Q. Wang, Experimental research on methane/air explosion inhibition using ultrafine water mist containing additive, *J. Loss Prev. Process Ind.*, 2016, **43**, 352–360.
- 17 P. G. Holborn, P. Battersby, J. M. Ingram, A. F. Averill and P. F. Nolan, Modelling the mitigation of hydrogen deflagrations in a vented cylindrical rig with water fog and nitrogen dilution, *Int. J. Hydrogen Energy*, 2013, **38**(8), 3471–3487.
- 18 A. U. Modak, A. Abbud-Madrid, J. Delplanque and R. J. Kee, The effect of mono-dispersed water mist on the suppression of laminar premixed hydrogen-, methane-, and propane-air flames, *Combust. Flame*, 2006, **144**(1–2), 103–111.
- 19 M. Gieras, Flame acceleration due to water droplets action, *J. Loss Prev. Process Ind.*, 2008, **21**(4), 472–477.
- 20 H. Cheikhravat, J. Goulier, A. Bentaib, N. Meynet, N. Chaumeix and C. E. Paillard, Effects of water sprays on flame propagation in hydrogen/air/steam mixtures, *Proc. Combust. Inst.*, 2015, **35**(3), 2715–2722.
- 21 M. Yu, A. An and H. You, Experimental study on inhibiting the gas explosion by water spray in tube, *J. China Coal Soc.*, 2011, **36**(3), 417–422.
- 22 H. K. Chelliah, A. K. Lazzarini, P. C. Wanigarathne and G. T. Linteris, Inhibition of premixed and non-premixed flames with fine droplets of water and solutions, *Proc. Combust. Inst.*, 2002, **29**(1), 369–376.
- 23 B. Pei, M. Yu, L. Chen, X. Zhu and Y. Yang, Experimental study on the synergistic inhibition effect of nitrogen and ultrafine water mist on gas explosion in a vented duct, *J. Loss Prev. Process Ind.*, 2016, **40**, 546–553.
- 24 B. Pei, M. Yu, L. Chen, F. Wang, Y. Yang and X. Zhu, Experimental study on the synergistic inhibition effect of gas-liquid two phase medium on gas explosion, *J. Loss Prev. Process Ind.*, 2017, **49**, 797–804.
- 25 J. Wang, Z. Huang, H. Kobayashi and Y. Ogami, Laminar burning velocities and flame characteristics of CO-H<sub>2</sub>-CO<sub>2</sub>-O<sub>2</sub> mixtures, *Int. J. Hydrogen Energy*, 2012, **37**(24), 19158–19167.
- 26 L. Qiao, C. H. Kim and G. M. Faeth, Suppression effects of diluents on laminar premixed hydrogen/oxygen/nitrogen flames, *Combust. Flame*, 2005, **143**(1), 79–96.
- 27 Y. Xie, J. Wang, N. Xu, S. Yu and Z. Huang, Comparative study on the effect of CO<sub>2</sub> and H<sub>2</sub>O dilution on laminar burning characteristics of CO/H<sub>2</sub>/air mixtures, *Int. J. Hydrogen Energy*, 2014, **39**(7), 3450–3458.
- 28 W. Kim and Y. Sato, Experimental study on self-acceleration in expanding spherical hydrogen-air flames, *Int. J. Hydrogen Energy*, 2018, **43**(27), 12556–12564.
- 29 J. Shan, W. Yan, L. Tao and W. Yun, Mechanism characteristics of CO<sub>2</sub> and N<sub>2</sub> inhibiting methane explosions in coal mine roadways, *J. China Coal Soc.*, 2013, **38**(3), 361–366.
- 30 X. Bao, F. Liu and Z. Sun, Study on Instability of Outwardly Propagating Spherical Premixed Flame, *J. Xihua Univ., Nat. Sci. Ed.*, 2014, 79–83.
- 31 G. E. Andrews, P. Herath and H. N. Phylaktou, The influence of flow blockage on the rate of pressure rise in Large L/D cylindrical closed vessel explosions, *J. Loss Prev. Process Ind.*, 1990, **3**(3), 291–302.
- 32 C. R. Bauwens, J. M. Bergthorson and S. B. Dorofeev, Experimental investigation of spherical-flame acceleration in lean hydrogen-air mixtures, *Int. J. Hydrogen Energy*, 2017, **42**(11), 7691–7697.
- 33 L. Qiao, Y. Gan, T. Nishiie, W. J. A. Dahm and E. S. Oran, Extinction of premixed methane/air flames in microgravity by diluents: effects of radiation and Lewis number, *Combust. Flame*, 2010, **157**, 1446–1455.
- 34 A. Yoshida, T. Okawa, W. Ebina and H. Naito, Experimental and numerical investigation of flame speed retardation by water mist, *Combust. Flame*, 2015, **162**(5), 1772–1777.

